New Mexico Geological Society

Downloaded from: https://nmgs.nmt.edu/publications/guidebooks/55

Initial paleoseismic and yydrogeologic assessment of the Southern Sangre de Cristo fault at the Taos Pueblo site, Taos County, New Mexico

K. I. Kelson, P. W. Bauer, S. D. Connell, D. W. Love, G. C. Rawling, and M. Mansell
2004, pp. 289-299. https://doi.org/10.56577/FFC-55.289

in:

Geology of the Taos Region, Brister, Brian; Bauer, Paul W.; Read, Adam S.; Lueth, Virgil W.; [eds.], New Mexico Geological Society 55 th Annual Fall Field Conference Guidebook, 440 p. https://doi.org/10.56577/FFC-55

This is one of many related papers that were included in the 2004 NMGS Fall Field Conference Guidebook.

Annual NMGS Fall Field Conference Guidebooks

Every fall since 1950, the New Mexico Geological Society (NMGS) has held an annual Fall Field Conference that explores some region of New Mexico (or surrounding states). Always well attended, these conferences provide a guidebook to participants. Besides detailed road logs, the guidebooks contain many well written, edited, and peer-reviewed geoscience papers. These books have set the national standard for geologic guidebooks and are an essential geologic reference for anyone working in or around New Mexico.

Free Downloads

NMGS has decided to make peer-reviewed papers from our Fall Field Conference guidebooks available for free download. This is in keeping with our mission of promoting interest, research, and cooperation regarding geology in New Mexico. However, guidebook sales represent a significant proportion of our operating budget. Therefore, only *research papers* are available for download. *Road logs*, *mini-papers*, and other selected content are available only in print for recent guidebooks.

Copyright Information

Publications of the New Mexico Geological Society, printed and electronic, are protected by the copyright laws of the United States. No material from the NMGS website, or printed and electronic publications, may be reprinted or redistributed without NMGS permission. Contact us for permission to reprint portions of any of our publications.

One printed copy of any materials from the NMGS website or our print and electronic publications may be made for individual use without our permission. Teachers and students may make unlimited copies for educational use. Any other use of these materials requires explicit permission.

This page is intentionally left blank to maintain order of facing pages.

INITIAL PALEOSEISMIC AND HYDROGEOLOGIC ASSESSMENT OF THE SOUTHERN SANGRE DE CRISTO FAULT AT THE TAOS PUEBLO SITE, TAOS COUNTY, NEW MEXICO

KEITH I. KELSON[1], PAUL W. BAUER[2], SEAN D. CONNELL[2], DAVID W. LOVE[2], GEOFFREY C. RAWLING[2], AND MARK MANSELL[2]

[1]William Lettis & Associates, Inc., 1777 Botelho Drive, Suite 262, Walnut Creek, CA 94596

[2]New Mexico Bureau of Geology and Mineral Resources, 801 Leroy Place, Socorro, NM 87801

ABSTRACT.—The most-recent surface-rupturing earthquake on the southern Sangre de Cristo fault at the Taos Pueblo site occurred about 10 to 30 ka, based on stratigraphic and soils relations in trench exposures. Detailed topographic surveys at the site show that the primary fault scarp, which is formed on late Pleistocene alluvial deposits, has about 3 m of net vertical tectonic displacement. A bevel in the scarp suggests that two surface ruptures occurred since deposition of the alluvial fan, each with about 1.5 m of vertical displacement. These displacements imply the occurrence of earthquakes having magnitudes in the range of **M**6.8 to **M**7.0. Stratigraphic relations exposed in a 30-m-long trench across the primary fault scarp show the presence of middle Pleistocene eolian and alluvial deposits faulted against late Pleistocene alluvial and colluvial deposits on the eastern, downthrown side of the fault. Stratigraphic evidence of surface-fault rupture includes scarp-derived colluvium and fissure-fill deposits that probably were deposited immediately following the surface rupture. The main fault strand consists of a primary west-dipping fault plane and secondary faulting in a 6-m-wide zone in the hanging wall. The fault zone contains multiple anastomosing strands in pervasively sheared alluvium, and probably has lower permeability than surficial deposits east of the fault, but higher permeability compared to deposits west of the fault. Calcium-carbonate cementation along fault planes in fine- and medium-grained deposits may be indicative of preferential groundwater flow downdip along the fault. Thus, major strands of the southern Sangre de Cristo fault probably provide preferential pathways for the downward flow of vadose-zone groundwater in unconsolidated near-surface deposits.

INTRODUCTION

The southern Sangre de Cristo fault is the most prominent rift-margin normal fault in the Rio Grande rift of northern New Mexico, and it plays a major role in both the tectonic and hydrogeologic setting of the Taos Plateau. The fault exhibits geomorphic evidence of several large earthquakes in late Quaternary time (Machette and Personius, 1984; Menges, 1988, 1990), and arguably is the most likely source of large earthquakes in northern New Mexico (Kelson and Olig, 1995; Wong et al., 1996; Machette et al., 1998). However, there are no detailed data on the timing of large, surface-rupturing earthquakes on the fault, although these data are critical for assessing the potential for future large earthquakes and the overall seismic hazard in northern New Mexico. In addition, the southern Sangre de Cristo fault traverses the eastern margin of the Taos Plateau, and juxtaposes crystalline and sedimentary bedrock in the mountains on the east against unconsolidated rift-fill deposits on the west. As a result, the fault is a primary structural discontinuity that likely affects groundwater flow in both the deep and shallow subsurface. Our trenching investigation described here provides information on large, geologically recent earthquakes on the southern Sangre de Cristo fault and documents fault characteristics in the shallow subsurface that help evaluate how the fault influences vadose-zone groundwater flow.

The 75-km-long southern Sangre de Cristo fault forms the eastern border of the actively subsiding San Luis Basin and is divided into five sections on the basis of fault-trace complexity and mountain-front and fault-scarp morphologic data (Menges, 1988; Machette et al., 1998; Fig. 1). This study focused on a site on the 14-km-long southern section of the fault (i.e., the Cañon

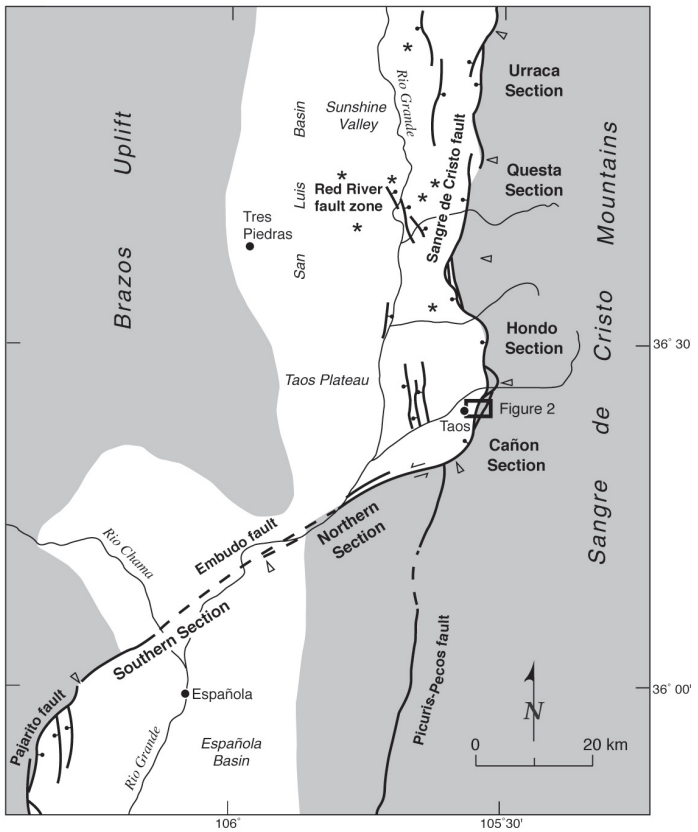

FIGURE 1. Generalized location map of the southern Sangre de Cristo fault in northern New Mexico, showing fault sections identified by Menges (1988) and Machette et al. (1998). Section boundaries marked by open triangles, and major volcanic centers marked by asterisks. Shaded area shows uplifted regions, non-shaded area shows rift-related basins.

section of Machette et al., 1998) (Fig. 1), where it shows geomorphic evidence of geologically recent, down-on-the-west surface rupture, including scarps on alluvial fans of various ages, air-photo lineaments, springs, and vegetation alignments. Topographic profiling of scarps on the Cañon section by Machette and Personius (1984) and Personius and Machette (1984) suggest a Holocene age (within the past 11,000 years) for the most-recent movement. Kelson (1986) mapped late Pleistocene alluvial deposits along this section, and Menges (1988, 1990) conducted detailed morphometric analyses of the range front and fault scarps. He suggested the possibility of early Holocene to latest Pleistocene movement along the Cañon section, with an estimated recurrence interval of about 10 to 50 ky between large surface ruptures. However, prior to our work, no paleoseismic trench investigations of the southern Sangre de Cristo fault had been conducted, and the timing of past surface fault ruptures was unknown. This study at the Taos Pueblo site is the first trenching study of the southern Sangre de Cristo fault in northern New Mexico, and it provides preliminary information on the late Pleistocene to Holocene history of large, surface-rupturing earthquakes on this part of the fault. We also document the fault's near-surface characteristics where it displaces unconsolidated surficial deposits, and speculate on the role the fault plays in shallow groundwater flow.

GEOLOGIC SETTING OF THE TAOS PUEBLO SITE

Detailed geologic mapping (Bauer and Kelson, 2002) indicates that the Taos Pueblo site is one of the best places to assess the earthquake history and near-surface characteristics of the southern Sangre de Cristo fault. We chose this site for investigation because: (1) geomorphic relations constrain the location of the main fault strand; (2) late Pleistocene alluvial deposits are preserved on the mountain-front piedmont; and (3) cultural disturbance is minimal. The site is on the west-sloping piedmont that flanks the Sangre de Cristo Mountains and consists of an alluvial apron derived from large and small drainages in the range (Fig. 2). The alluvial deposits are composed primarily of gravel and sand derived from erosion of Pennsylvanian-age sandstone, siltstone, and minor conglomerate and limestone in the Sangre de Cristo Mountains (Bauer and Kelson, 2002). Notably, the pres-

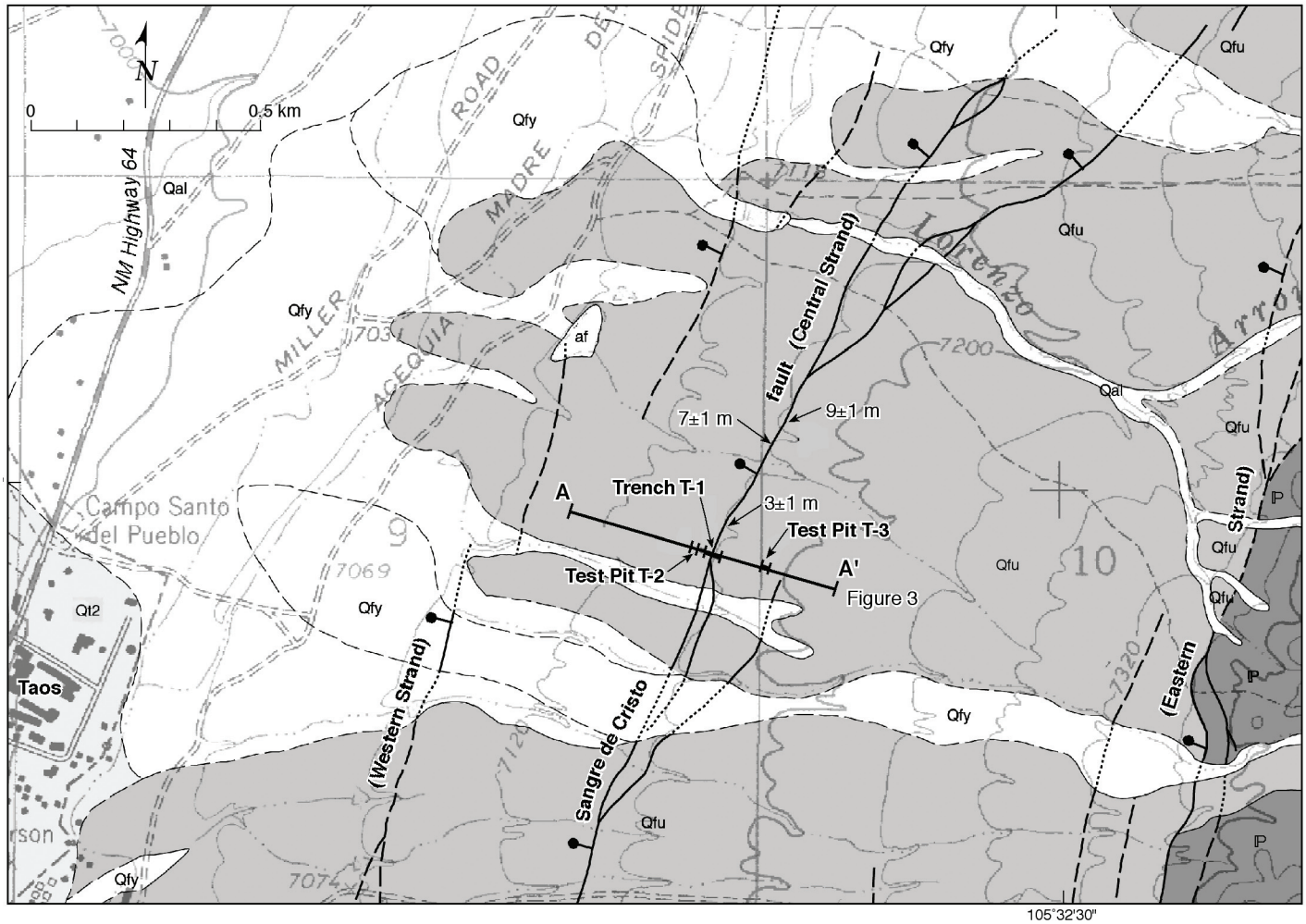

FIGURE 2. Geologic map of the western flank of the Sangre de Cristo Mountains near Taos showing location of the Taos Pueblo trench site. Geology from Bauer et al. (2001); map units are: af = artificial fill, Qal = Holocene alluvium, Qfy = Holocene and latest Pleistocene alluvial deposits (multiple fan lobes shown), Qfu = Pleistocene alluvial deposits, undifferentiated (light stipple), Qt2 = middle to early (?) Pleistocene alluvium, P = Pennsylvanian bedrock (dark stipple). Values shown are displacements based on fault scarp topographic profiles.

ence of limestone clasts in the alluvial deposits (albeit as a minor component) provides a source of calcium carbonate that, in addition to eolian influx, probably influences the morphology and rate of development of calcic soils at the site.

Near the site (Fig. 2), the southern Sangre de Cristo fault consists of three main fault strands, including: (1) an eastern strand delineated by a break-in-slope at the base of the bedrock range front east of the site; (2) a central strand marked by a prominent west-facing scarp at the trench site, and (3) a western strand associated with a broad, west-facing scarp about 0.6 km west of the trench site (Bauer and Kelson, 2002). Based on geologic mapping and scarp geomorphology, the central strand is the primary fault strand that has been active in late Quaternary time. Trench T-1 crossed the prominent west-facing scarp on the central strand. Directly south of the trench site, this strand splits into two strands and is marked by a subtle splay fault east of the trench site (Fig. 2). Detailed field mapping shows that fault scarps on late Quaternary deposits are discontinuous on the eastern strand, and scarps on the western fault strand (west of the trench site, Fig. 2) are subtle, broad, and much less prominent than the scarp at the trench site. Based on the geomorphic expression of the three scarps near the trench site, we consider the central strand to be the strand that has been most active in late Quaternary time in the site vicinity.

The prominent fault scarp at the site is on "undifferentiated Pleistocene alluvial-fan deposits" (map unit Qfu, Bauer and Kelson, 2002), which consists of coalescent alluvial fans (Fig. 2). These deposits are distinguished from "young alluvial-fan deposits" (map unit Qfy, Fig. 2), which are topographically inset into unit Qfu, have less soil development, and generally are associated with present-day arroyos or areas of active alluviation. Bauer and Kelson (2002) estimated that unit Qfy is Holocene to latest Pleistocene in age, and that unit Qfu is middle to late Pleistocene in age. Near the trench site, fault scarps are present on three different alluvial surfaces associated with unit Qfu, each of which is displaced a different amount. Detailed topographic surveys of the site using a differentially corrected global positioning satellite system shows that the primary scarp has about 3 m of net vertical tectonic displacement (NVTD) (Fig. 3). Topographic profiles show that the alluvial surface 300 m north of the trench site has a NVTD of 7 ± 1 m, and the fan surface about 400 m north of the site has a NVTD of 9 ± 1 m (Fig. 2; Bauer et al., 2001). These greater scarp heights on progressively older fan deposits are evidence of multiple late Quaternary surface ruptures on the central fault strand.

The main scarp at the Taos Pueblo site has a distinct bevel that may indicate it was formed by multiple surface-rupturing earthquakes. As shown on Figure 3C, a steep, central part of the scarp is flanked by sections that are less steep. Projecting the gradients of these bevels suggests that the central part of the scarp has about 1.5 m of NVTD, whereas the NVTD for the entire scarp is about 3 m (Fig. 3C). These relations suggest that two surface ruptures have offset the alluvial surface, each having about 1.5 m of NVTD. On the basis of these data, we speculate that two past surface ruptures have occurred since the deposition of the late Pleistocene alluvial fan. These displacements are consistent

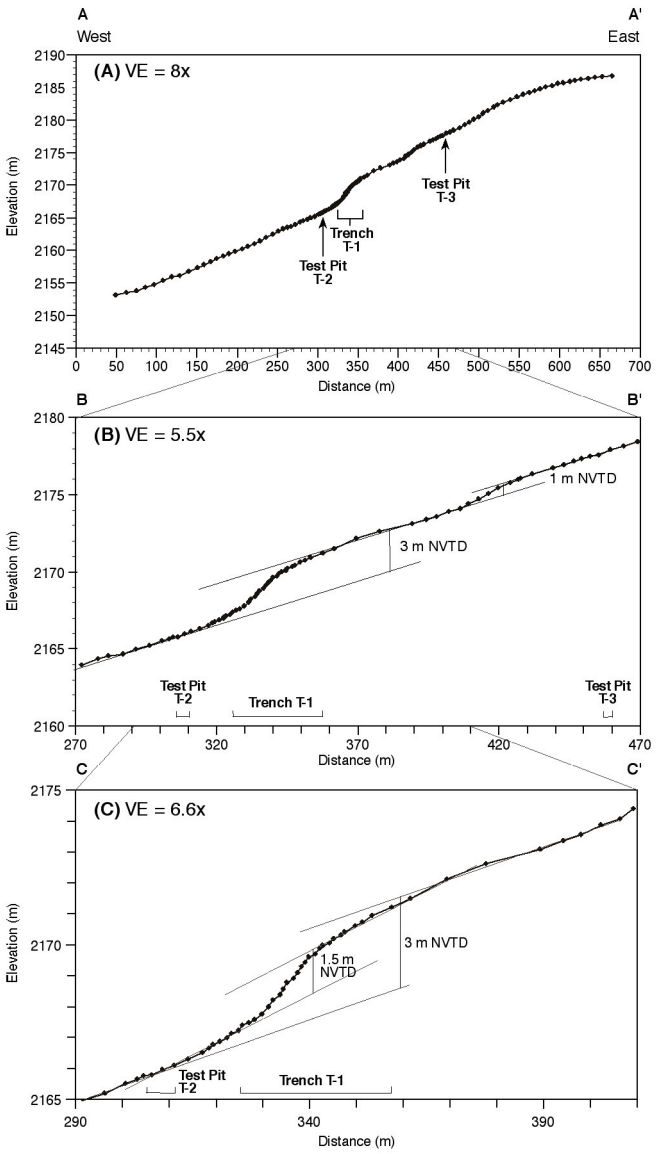

FIGURE 3. Topographic profiles across the southern Sangre de Cristo fault at the Taos Pueblo trench site, showing net vertical tectonic displacement (NVTD). Profiles AA' through CC' show progressively more detail across main fault strand. A bevel in profile CC' may be evidence of multiple surface ruptures.

with large earthquakes having magnitudes in the range of **M**6.8 to **M**7.0 (Wells and Coppersmith, 1994).

TRENCH STRATIGRAPHY AND STRUCTURE

Trench T-1 was excavated across the west-facing fault scarp on late Pleistocene alluvial deposits (unit Qfu, Fig. 2). To assess the characteristics of near-surface soils on both sides of the fault, we excavated two test pits: T-2 on the downthrown (western) side of the fault and T-3 on the upthrown (eastern) side of the fault (Fig. 2). Faulted alluvial deposits and scarp-derived colluvial deposits exposed in these excavations provide information on the number

and timing of surface ruptures and thus the late Quaternary history of the fault (Kelson et al., 2004).

Soil profiles described in the test pits and the trench provide a means to correlate deposits across the fault and to estimate deposit ages (Gile et al., 1981; Machette, 1985; McFadden et al., 1989). We described the soil-profile morphology using a standard system of diagnostic criteria and nomenclature developed by the Soil Conservation Service (Soil Survey Staff, 1992, 1993), with modifications after Birkeland (1999). Geomorphic and soil-based alluvial chronologies in the region provide correlative age constraints to help estimate ages of soil-bounded alluvial deposits in our excavations (e.g., Gile et al., 1981; Machette, 1985; Kelson, 1986; Pazzaglia and Wells, 1990; McDonald et al., 1996; Connell and Wells, 1999; Drakos and Reneau, 2003). Soils in the study area contain horizons with secondary accumulations of pedogenic clay and carbonate. The carbonate accumulations range from disseminated calcium carbonate to stage I to III+ carbonate morphology. In general, soils that exhibit stage I to II carbonate morphology are considered to be early Holocene to latest Pleistocene in age, and soils that exhibit stage III and IV carbonate morphology are considered to be middle Pleistocene in age (e.g., Machette, 1985; Kelson, 1986; Pazzaglia and Wells, 1990; McDonald et al., 1996).

Trench Stratigraphy

Trench T-1 exposed a sequence of Pleistocene and Holocene alluvial, colluvial, and possibly eolian deposits (Fig. 4; Appendix A). Deposits east of the fault scarp consist of primarily massive silty sand (of probable eolian and minor fluvial origin), which is overlain by coarse alluvial deposits from the Sangre de Cristo Mountains. For ease of description, we herein refer to the possible eolian deposits as unit 1 and the coarse alluvial deposits collectively as unit 2 (Fig. 4). On the western side of the fault, the deposits consist of coarse- and fine-grained alluvial deposits (units 3 and 4), which are overlain by carbonate-cemented alluvium or colluvium (units 5 and 6). Units 7 and 8 are vertically oriented and may be fault gouge or fissure fills related to surface ruptures. Overlying these deposits is scarp-derived colluvium, including a coarse proximal colluvium (unit 9) that grades upward into finer-grained distal colluvium (unit 10). The uppermost deposit in the trench is a coarse- to medium-grained gravelly and sandy colluvium that is a result of active transport of material down the fault scarp (unit 11). At present, we do not have numerical or correlative age-estimates for the deposits exposed at the Taos Pueblo site, so we base rough age estimates for the surficial deposits (as given below) on the characteristics of soils in the deposits (Appendix B), their stratigraphic position, and the site geomorphology.

Unit 1, the oldest deposit in the trench (Fig. 4), consists primarily of massive silt and clay (Appendix A) that we interpret as eolian deposits along the Sangre de Cristo mountain front. The uppermost part of unit 1 contains thin clayey sand beds, suggesting minor re-working of the deposit by small channels. On the basis of its stratigraphic position, we interpret unit 1 to be at least middle Pleistocene in age. Unit 2 consists of coarse-grained gravel that fills several alluvial channels cut into the underlying eolian sand, and has crudely imbricated sandstone and siltstone clasts as much as 36 cm in diameter. In test pit T-3, this older alluvium is the parent material in which a carbonate-cemented soil horizon with stage III+ morphology has formed (Appendix B). Locations of the gravel channel margins in both walls of trench T-1 suggest northwesterly to northerly flow directions that are not related to modern channel orientations or incised-channel topography. These deposits represent proximal to medial piedmont alluvial deposits derived from the Sangre de Cristo Mountains to the southeast. On the basis of well-developed soil characteristics and stratigraphic position, we interpret unit 2 to be middle Pleistocene in age.

Units 3 and 4 are alluvial deposits exposed only on the western (downthrown) side of the fault in trench T-1 and test pit T-2 (Fig. 4). Unit 3, which is the lowest stratigraphic unit exposed on the downthrown side of the fault, consists of sandy gravel with clasts as much as 30 cm in diameter, grading upward into gravelly sand (Appendix A). Unit 3 grades upward into unit 4, which is a silty sand that has few or no gravel clasts. Unit 4 contains an intersecting pattern of subhorizontal and subvertical calcium-carbonate stringers that likely are related to vadose-zone groundwater flow. Collectively, units 3 and 4 comprise a fining-upward alluvial sequence that probably was deposited as part of the alluvial apron flanking the Sangre de Cristo Mountains. These deposits have moderately developed calcic soils with stage III carbonate morphology (Appendix B) and are inferred to be middle Pleistocene in age.

Units 5 and 6 are exposed only on the western (downthrown) side of the fault in trench T-1 and test pit T-2 (Fig. 4) and consist of a second fining-upward alluvial sequence. Unit 5 consists of sand and gravel, with a greater number and size of clasts adjacent to the main fault strand (Fig. 4b; Appendix A). Unit 5 also contains slightly more clasts directly west of the secondary fault strand (Station 21 m, Fig. 4b). Unit 5 grades upward into unit 6, which is a light pink-colored clayey sand with locally discontinuous stone lines. Unit 6 is strongly effervescent and pervasively cemented with calcium carbonate. Units 5 and 6 likely also represent deposition as part of the alluvial apron along the piedmont of the Sangre de Cristo Mountains. However, we also consider the possibility that these deposits were shed from a fault scarp formed by surface fault rupture. In this case, unit 5 is the coarse, proximal scarp-derived colluvium, and unit 6 is the relatively fine-grained distal colluvium. The Sangre de Cristo fault clearly displaces both of these deposits, and well-defined fault planes are marked by rotated clasts and shear fabric in these units. Stage III+ carbonate morphology in the soil developed in these deposits (Appendix B) suggests that the deposits are middle or possibly late Pleistocene in age.

Unit 7 consists of two separate, near-vertical bodies of sand and gravel similar in size and sorting to units 4, 5 and 6, and is associated with strands of the Sangre de Cristo fault in trench T-1 (Figs. 4 and 5). Along the main fault strand (Stations 25 to 26 m; Fig. 5), unit 7 is loose, pervasively sheared and most clasts have near-vertical orientations. This unit likely is fault gouge produced by shearing and tectonic deformation of units 2 and 5. Along the

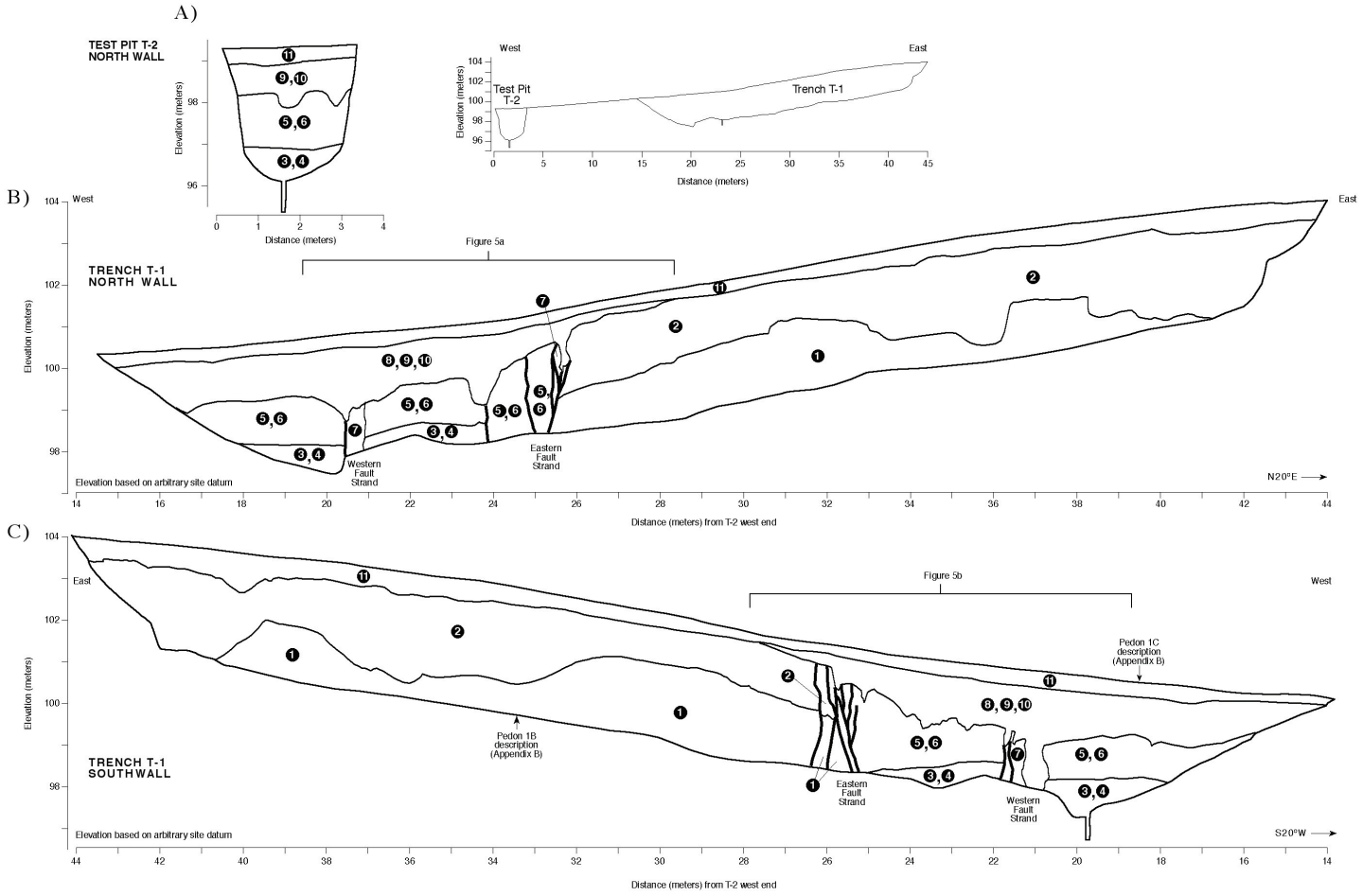

FIGURE 4. Simplified maps of (a) southern wall of test pit T-2, (b) northern wall of trench T-1, and (c) southern wall of trench T-1 (after Kelson et al., 2004). Unit descriptions are in Appendix A; soil characteristics are in Appendix B.

secondary fault strand (Station 21 m, Figs. 4 and 5), unit 7 likely is fault gouge associated with deformation of units 4, 5 and 6 during movement along the secondary fault strand. Alternatively, unit 7 at Station 21 m may be fill deposited in an open fissure that formed during a surface rupture.

We interpret units 8, 9 and 10 to be local deposits that accumulated along the fault scarp following the most-recent surface rupture. Unit 8 consists of discontinuous sand and gravel deposits adjacent to either primary or secondary fault strands. Gravel clasts in this unit commonly have near-vertical orientations and are similar in size and rounding to those in adjacent deposits (i.e., units 2 or 6), which are the likely sources of unit 8. The cross-sectional shape of unit 8 suggests that it was deposited in open fissures or depressions along the fault, and we interpret this unit to be a fissure-fill deposit derived from adjacent units 4 to 7. Unit 8 grades upward into unit 9, which pinches out to the east and buries the lower and middle parts of the old fault scarp (Fig. 4). Near the fault, the base of unit 9 is sandy gravel, but it is finer upward and away from the fault. The size and rounding of the gravel clasts is consistent with derivation from the older alluvium that forms the scarp crest (unit 2), and unit 9 clearly is coarser where it directly overlies this alluvium (Fig. 4). Gravel clasts within unit 9 are oriented parallel to the depositional slope, which also supports our interpretation that this deposit is the proximal scarp-derived colluvium. Unit 9 grades upward into unit 10, which contains fewer gravel clasts and is confined to the downthrown side of the fault. We interpret unit 10 to be distal scarp-derived colluvium. The moderately developed soil in units 9 and 10 includes a Btk horizon and stage I calcium-carbonate morphology (Appendix B). These soil characteristics suggest a latest Pleistocene age for these deposits, and we speculate that they are on the order of 10 to 30 ka.

The uppermost deposit in trench T-1 is unit 11 which unconformably overlies unit 2 east of the fault and units 9 and 10 west of the fault (Fig. 4). This unfaulted deposit consists of silty sand to clayey sand with some gravel clasts. The gravel distribution in unit 11 directly reflects local underlying units, such that unit 11 contains abundant gravel where it overlies gravelly units 2 and 9, and contains few clasts where it overlies fine-grained unit 10 (Fig. 4). We interpret unit 11 to be late Holocene hillslope colluvium that is in transit on the present-day fault scarp.

Trench Geologic Structure

Trench T-1 exposed the primary strand of the Sangre de Cristo fault, which is approximately 6 m wide and contains a well-developed west-dipping eastern fault strand and a secondary, near-vertical zone of fault gouge and fissure-fill deposits (Figs. 4 and 5). These two zones of deformation likely merge at a shallow depth below the trench. The eastern fault strand (at about Station 26 m) dips about 70˚ west, and juxtaposes middle Pleistocene eolian deposits and alluvium on the east (units 1 and 2) against middle to late Pleistocene alluvium (units 5 and 6) on the west (Figs. 4 and 5). Gravel beds in unit 2 are warped into the fault zone and are subparallel to the fault at lower structural levels. Within the fault zone, alluvium is sheared and mixed; unit 7 at Station 26 m is mapped as fault gouge developed in the unconsolidated alluvial gravel. The fault zone contains multiple anastomosing strands in the sheared alluvium, with individual strands commonly bordering lenticular bodies of sheared sediments. In addition, the fault zone includes multiple vertical strands in units 1 and 2 in the footwall (Fig. 5b), which progressively decrease in density and degree of shearing to the east.

The western zone of deformation (at about Station 21 m) has about 40 cm of vertical displacement of units 5 and 6 (Figs. 4 and 5). Although the western fault strand does not displace unit 8, this unit is spatially associated with the western fault strand. On the southern wall of the trench, unit 8 is a loose, near-vertical tabular body that we interpret as a fissure fill. On the northern wall of trench T-1, unit 8 has a triangular shape, suggesting that the fissure was laterally discontinuous along the fault rupture. As noted above, none of the fault strands exposed in Trench T-1 extends into unit 8 or overlying surficial deposits, indicating that this fissure opened during the most-recent faulting event.

The northern trench wall exposed a complex pattern of deformation on the downthrown block (Fig. 5a). Near Station 25 m, a near-vertical down-on-the-west fault juxtaposes units 5 and 6. In addition, at about Station 24 m, the trench exposed a loose, mixed zone that we mapped as a series of animal burrows and fissure fills (unit 8). In this area, unit 5 has a net down-on-the-east displacement, indicating the presence of a 1.5-m-wide graben in the downthrown block adjacent to the eastern fault. In the graben, unit 5 contains abundant near-vertical stringers of calcium carbonate that probably reflect preferential groundwater percolation along fractures and/or shear planes in the sediment. On the southern trench wall, there is no evidence of this graben, because the base of unit 5 extends continuously across the entire exposure. The absence of the graben on the southern trench wall indicates that it is a laterally discontinuous feature formed during a surface-rupturing earthquake.

PALEOSEISMOLOGIC INTERPRETATIONS

On the basis of the stratigraphy in Trench T-1, units 8, 9 and 10 were deposited locally along the scarp following the most recent surface rupture. The location and character of unit 8 suggest that it was deposited soon after the surface rupture, and filled surface fissures, cracks, and depressions locally along the base of the fresh fault scarp. Similarly, unit 9 was deposited soon after the rupture, as the steep, fresh scarp degraded and shed colluvium to the west. This colluvium included coarse gravel derived from uplifted older alluvium (unit 2) that was exposed in the scarp face, and perhaps remnants of units 5 and 6 if they were present on the scarp at the time of the earthquake. Further degradation of the scarp produced unit 10, and later unit 11. The moderately developed soil on units 9 and 10 suggests a latest Pleistocene age for the deposit, which we speculate to be on the order of about 10 to 30 ka. Because these units probably were deposited within several hundreds to a few thousands of years after the surface rupture, the most-recent large earthquake on the southern Sangre de Cristo fault at the Taos Pueblo site probably occurred between about 10 to 30 ky ago. Refining this age estimate requires additional studies that are beyond the scope of our initial study described here.

On the basis of detailed topographic profiling (Fig. 3), we estimate that the most-recent surface rupture produced approximately 1.5 m of NVTD at the site. This amount is consistent with stratigraphic relations mapped in trench T-1. For example, the thickness of the scarp-derived colluvium (units 9 and 10, Figs. 4 and 5) is about 0.6 to 1.2 m, or roughly half of the estimated down-on-the-west NVTD. We interpret units 5 and 6 to be older scarp-derived colluvium, but because the age of these deposits is poorly constrained, the trench provides no conclusive information on the timing of surface ruptures that occurred prior to the most-recent surface-rupturing earthquake.

HYDROGEOLOGIC INTERPRETATIONS

The geometry and style of deformation in the fault zone may influence the flow of shallow groundwater along or across the Sangre de Cristo fault. Characteristics of deformed sediments in the trench include: (1) clasts that are rotated to be subparallel to the fault; (2) foliations in clay and clayey sand; (3) drag and incorporation of strata into the fault zone; and (4) tectonic mixing of different sediment types. In addition, calcium-carbonate cement is common along fault planes in fine- and medium-grained deposits and as intersecting subhorizontal and subvertical stringers that likely are related to vadose-zone groundwater flow.

Based on these observations, we believe that the hydrologic properties of the Sangre de Cristo fault are grossly similar to other faults in the rift that have been studied in detail, such as the Sand Hill fault near Albuquerque, New Mexico (Rawling et al., 2001). Drag and mixing of sand and clay in the fault zone creates a heterogeneous fault-zone material that is generally less porous than the original, undeformed deposits. Usually the hydraulic conductivity of such a fault zone in saturated conditions (i.e., below the water table) is less than the conductivity of adjacent sediments, especially gravel and coarse sand (Rawling et al., 2001). Alternatively, in well-cemented sediments, the saturated hydraulic conductivity of a fault zone may be higher than adjacent undeformed material because of tectonic fractures (such as in unit 6, Figs. 4 and 5). In vadose-zone conditions (i.e., above the water table), the reduction of porosity in poorly lithified sediments resulting from fault deformation commonly results in higher unsaturated hydraulic conductivity relative to adjacent gravels and coarse

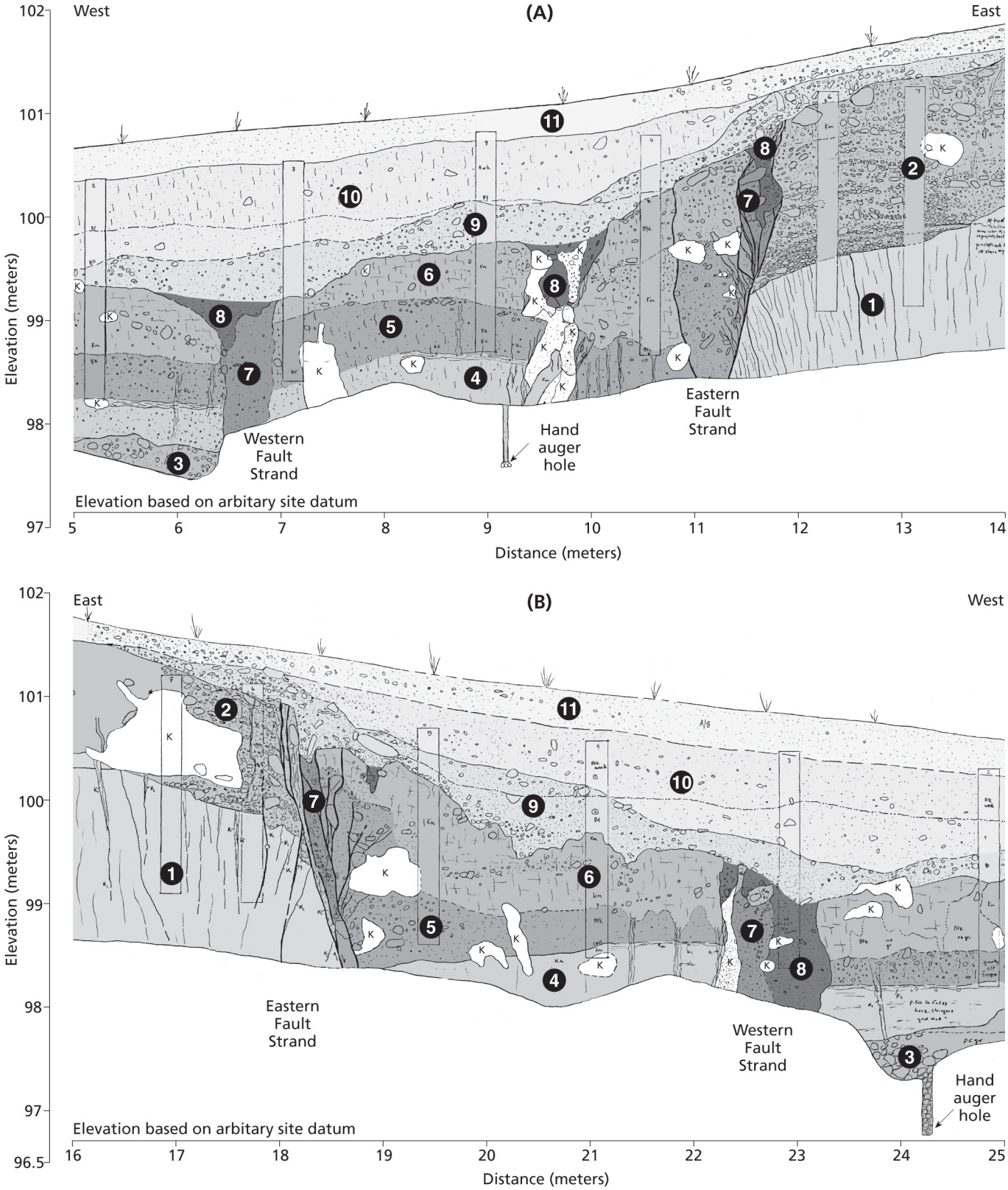

FIGURE 5. Detailed maps of Sangre de Cristo fault exposed in (a) northern wall and (b) southern wall of trench T-1, Taos Pueblo site. Unit descriptions are in Appendix A; K = krotovina (bioturbation). See Plate 9 for color figure of profiles.

sands (Sigda and Wilson, 2003). In this case, the fault may be a preferential pathway for downward-percolating surface waters to flow through the vadose zone.

In trench T-1, the uppermost part of the fault zone places unit 6 on the west against unit 2 on the east (Figs. 4 and 5). Unit 6 is pervasively cemented with pedogenic calcium carbonate and probably has low permeability, whereas unit 2 is loose alluvium locally that probably has high saturated permeability. The fault zone in trench T-1 is a mixture of these sediments (unit 7), which probably has variable permeability as a result of tectonic mixing and incorporation of blocks and clasts of the adjacent sediments. In general, the fault zone probably has a lower saturated permeability than undeformed parts of the loose alluvial gravel (unit 2), but higher saturated permeability than the undeformed cemented, fine-grained alluvium on the western side of the fault (unit 6; Figs. 4 and 5). In unsaturated conditions, the fault-zone permeability may be higher than that of unit 2. Thus, the fault zone may be a preferential flow pathway downward from the surface under both saturated and unsaturated conditions. In addition, the bulk permeability of the fault zone is likely to be anisotropic, such that saturated permeability is lower across the fault than down the fault's dip, because elongate pods of coarse sediment in the fault may provide high permeability, down-dip pathways. Local cementation along the fault in trench T-1 may be evidence of preferential flow along the fault.

In the upper part of the trench, the throw on the fault is small, but at greater depths the fault zone has experienced multiple ruptures and fault-zone structures are likely to be better developed. In particular, if a continuous, relatively impermeable clay-rich gouge zone has formed at depth, the gouge will be a significant barrier to horizontal groundwater flow (Rawling et al., 2001). Based on the distribution of cementation in trench T-1, percolating waters probably flow preferentially down-dip along the fault. Also, where the fault is traversed by active arroyos developed on the alluvial fan, these drainages probably provide surface water to the fault zone during flood events. Where active arroyos cross the fault, surface water and shallow groundwater that encounter the fault zone are likely diverted downward because the fault is a relatively permeable conduit.

CONCLUSIONS

The primary goals of this investigation were to: (1) develop information on large, geologically recent earthquakes on the southern Sangre de Cristo fault; and (2) document shallow subsurface characteristics of the fault to help evaluate the influence of the fault on vadose zone groundwater. The southern Sangre de Cristo fault has clear geomorphic evidence of geologically recent surface rupture, including scarps on alluvial fans of various ages, air-photo lineaments, springs, and vegetation alignments. Detailed topographic surveys of the site show that the primary fault scarp across the late Pleistocene alluvial surface has about 3 m of net vertical tectonic displacement. Progressively greater displacements of older alluvial surfaces suggest that the fault has produced multiple surface ruptures during the late Pleistocene. In addition, a distinct bevel in the scarp profile at the trench site suggests the occurrence of two surface ruptures since deposition of the alluvial fan, each having about 1.5 m of vertical displacement. These displacements are consistent with large earthquakes in the range of **M**6.8 to **M**7.0 (Wells and Coppersmith, 1994).

Stratigraphic relations in the trench across the fault scarp show that middle Pleistocene eolian and alluvial deposits on the eastern, upthrown side of the fault are faulted against probable late Pleistocene alluvial and colluvial deposits on the western, downthrown side. Stratigraphic evidence of surface-fault rupture includes scarp-derived colluvium on the downthrown side of the fault, which includes fissure-fill and proximal colluvium that probably were deposited shortly after the surface rupture. We interpret that the moderately developed soil on this colluvial package, including soil Btk horizons and stage I calcium-carbonate accumulation, represents about 10 to 30 ky of soil development. Thus, our trench at the Taos Pueblo site suggests that the most-recent surface rupture along the southern Sangre de Cristo fault occurred between about 10 and 30 ka. Geologic evidence of previous faulting exists in the form of well-developed fault gouge, an older sequence of possible proximal and distal scarp colluvium, and fault-scarp morphology, but the timing of this earlier deformation is unconstrained.

The main fault strand at the trench site consists of a primary west-dipping fault plane and secondary faulting within a 6-m-wide zone in the hanging wall. The trench exposed a local graben at the base of the scarp. The primary fault zone consists of multiple anastomosing strands within the sheared alluvium, with strands commonly bordering lenticular bodies of sheared sediments. Pervasive shearing in the fault zone probably generated a zone of low saturated permeability compared to coarse alluvium east of the fault, but a zone of high saturated permeability compared to cemented alluvial deposits west of the fault. Bulk permeability in the fault zone likely is anisotropic with greater permeability downward rather than across the fault. Several near-vertical fractures in the fault zone are associated with calcium-carbonate accumulations, suggesting that meteoric water preferentially percolates downward along the fractures. Thus, relations in the trench suggest that major strands of the southern Sangre de Cristo fault can be preferential pathways for the downward flow of vadose-zone groundwater in unconsolidated near-surface sediments.

ACKNOWLEDGMENTS

This investigation was conducted collaboratively between the New Mexico Bureau of Geology and Mineral Resources (Dr. P. Scholle, Director) and William Lettis & Associates, Inc. This project was supported, in part, by Grant # EMT-2003-GR-0003-EQ2 awarded by the Federal Emergency Management Agency. This publication does not necessarily reflect FEMA's views. We thank Ms. Susan Walker of the New Mexico Department of Public Safety for providing matching funds for this effort and for visiting the site during the investigation. Michael Machette (USGS, Denver) graciously visited the trench and mapped key parts of the fault trench. William White and Christopher Banet (Bureau of Indian Affairs, Albuquerque) provided technical input on the

trench exposure and soil stratigraphy, and augered into the trench floor to provide additional stratigraphic data. Anthony Crone (USGS), John Baldwin (William Lettis & Associates, Inc.), and Bruce Harrison (New Mexico Tech) provided excellent technical comments that improved the paper. This investigation could not have been completed without the efforts and foresight of Nelson Cordova (Taos Pueblo Water Rights), and we are very grateful for his help and support. In addition, we would like to thank Taos Pueblo Warchief Lujan, his staff assistant Louis Zamora, and Tribal backhoe operator John Romero, for help in getting the project approved and completed.

REFERENCES

Bauer, P.W. and Kelson, K.I, 2002, Geology of the Taos 7.5-minute quadrangle, Taos County, New Mexico: New Mexico Bureau of Geology and Mineral Resources, Open-File Digital Geologic Map OF-DM 43, scale 1:24,000.

Birkeland, P.W., 1999, Soils and geomorphology: Oxford University Press, New York, 430 p.

Connell, S.D., and Wells, S.G., 1999, Pliocene and Quaternary stratigraphy, soils, and tectonic geomorphology of the northern flank of the Sandia Mountains, New Mexico: implications for the tectonic evolution of the Albuquerque Basin: New Mexico Geological Society, 50th Field Conference, Guidebook, p. 379-391.

Drakos, P.G., and Reneau, S.L., 2003, Surficial units and processes associated with archaeological sites in selected land conveyance parcels, Los Alamos National Laboratory: Glorieta Geosciences, Inc., unpublished Technical Report, 21 p., 5 tables.

Gile, L.H., Hawley, J.W., and Grossman, R.B., 1981, Soils and geomorphology in the Basin and Range area of southern New Mexico-Guidebook to the Desert Project: New Mexico Bureau of Mines and Mineral Resources Memoir 39, 222 p.

Kelson, K.I., 1986, Long-term tributary adjustments to base-level lowering northern Rio Grade rift, New Mexico: [M.S. thesis]: Albuquerque, University of New Mexico, 210 p.

Kelson, K I., Bauer, P.W., Love, D., Connell, S.D., Mansell, M. and Rawling, G.C., 2004, Initial paleoseismic and hydrologic assessment of the southern Sangre de Cristo fault at the Taos Pueblo site, Taos, New Mexico: New Mexico Bureau of Geology and Mineral Resources, Open-file Report 476, 46 p.

Kelson, K.I., and Olig, S.S., 1995, Estimated rates of Quaternary crustal extension in the Rio Grande rift, northern New Mexico: New Mexico Geological Society, 46th Field Conference, Guidebook, p. 9-12.

Machette, M.N., 1985, Calcic soils of the southwestern United States, *in* Weide, D.L., and Faber, M.L., eds., Soil and Quaternary geology of the southwestern United States: Geological Society of America Special Paper 203, p. 1-4.

Machette, M.N., and Personius, S.F., 1984, Quaternary and Pliocene faults in the eastern part of the Aztec quadrangle and the western part of the Raton quadrangle, northern New Mexico, U.S. Geological Survey Map MF-1465-B, scale 1:250,000.

Machette, M.N., Personius, S.F., Kelson, K.I., Dart, R.L., and Haller, K.M., 1998, Map and data for Quaternary faults in New Mexico: U.S. Geological Survey Open-file Report 98-521, 443 p.

McDonald, E.V., Reneau, S.L., and Gardner, J.N., 1996, Soil-forming processes on the Pajarito Plateau: investigation of a soil chronosequence in Rendija Canyon: New Mexico Geological Society, 47th Field Conference, Guidebook, p. 367-374.

McFadden, L.D., Ritter, J.B., and Wells, S.G., 1989, Use of multiparameter relative-age methods for age estimation and correlation of alluvial fan surfaces on a desert piedmont, eastern Mojave Desert, California: Quaternary Research, v. 32, p. 276-290.

Menges, C.M., 1988, The tectonic geomorphology of mountain front landforms in the northern Rio Grande rift, [Ph.D. dissertation]: Albuquerque, University of New Mexico, 140 p.

Menges, C.M., 1990, Late Cenozoic rift tectonics and mountain-front landforms of the Sangre de Cristo Mountains near Taos, northern New Mexico: New Mexico Geological Society, 41st Field Conference, Guidebook, p. 113-122.

Munsell Company, 1992, Soil Color Chart: New York, Munsell Company, Kollmorgen Instruments Corporation.

Pazzaglia, F.J., and Wells, S.G., 1990, Quaternary stratigraphy, soils and geomorphology of the northern Rio Grande rift: New Mexico Geological Society, 41st Field Conference, Guidebook, p. 423-430.

Personius, S.F., and Machette, M.N., 1984, Quaternary faulting in the Taos Plateau region, northern New Mexico: New Mexico Geological Society, 35th Field Conference, Guidebook, p. 83-90.

Rawling, G.C., Goodwin, L.B. and Wilson, J. L. 2001, Internal architecture, permeability structure, and hydrologic significance of contrasting fault-zone types: Geology v. 29, no. 1, 43-46 p.

Sigda, J.M., and Wilson, J.L. 2003, Are faults preferential flow paths through semiarid and arid vadose zones?: Water Resources Research v. 39, no. 8, doi:10.1029/2002WR001406.

Soil Survey Staff, 1992, Keys to soil taxonomy: U.S. Department of Agriculture Soil Management Support Services Technical Monograph Number 19, 541 p.

Soil Survey Staff, 1993, Soil survey manual: U.S. Department of Agriculture Handbook Number 18, 437 p.

Wells, D.L., and Coppersmith, K.J., 1994, New empirical relationships among magnitude, rupture length, rupture width, rupture area, and surface displacement: Bulletin of Seismological Society of America, v. 84, no. 4, p. 974-1002.

Wong, I.G., Kelson, K.I., Olig, S., Bott, J., Green, R., Kolbe, T., Hemphill-Haley, M., Gardner, J., Reneau, S., and Silva, W., 1996, Earthquake potential and ground shaking hazard at the Los Alamos National Laboratory, NM: New Mexico Geological Society, 47th Field Conference, Guidebook, p. 135-142.

APPENDIX A: DESCRIPTIONS OF TRENCH UNITS

Unit 11: Holocene colluvium; (7.5YR4/4) SILTY SAND to CLAYEY SAND. Fine to coarse sand; subrounded to subangular gravel as much as 5 cm; 20 to 30% gravel between stations 26 and 29 m; < 5% gravel west of station 215 m grading to no gravel west of station 21 m; poorly sorted; dry, slightly hard to loose; bioturbated; footwall exposures contain clasts of underlying pedogenic stage III soil of unit 2; upper 10 to 20 cm contains no pedogenic calcium carbonate; lower part ranges to stage 1; locally overlies hearth and deposit containing black smudge-ware potsherd; (ACTIVE HILLSLOPE COLLUVIUM).

Unit 10: Late Pleistocene colluvium. Brown to light brown (7.5YR 5/4 to 7.5YR 6/4) SANDY CLAY. Fine to coarse sand; subrounded to subangular gravel as much as 10 cm; as much as 5% gravel, with more gravel closer to fault and in upper parts of unit; locally contains discontinuous, gently west-dipping gravel stone lines; poorly sorted; dry, slightly hard to hard; contains as much as stage I+ calcium carbonate (soil Btk horizons); calcium carbonate nodules; slightly effervescent; gradual smooth basal contact; (TECTONIC SCARP-DERIVED DISTAL COLLUVIUM).

Unit 9: Late Pleistocene colluvium. Reddish yellow (7.5YR 6/6) SANDY CLAY to SANDY GRAVEL. Fine to coarse sand; subrounded to subangular gravel as much as 40 cm; 20 to 30% gravel in eastern part of unit (near stations 24 to 28 m); 5 to 15% gravel in western part of unit (west of station 24); slightly smaller gravel clasts progressively westward; smaller gravel clasts progressively upward, especially near stations 23 to 26 m (adjacent to primary fault); clast rounding, size, lithology, and location suggests derivation from unit 2 on hanging wall; locally contains discontinuous, gently west-dipping gravel stone lines; poorly sorted; dry, hard; contains stage I+ calcium carbonate (soil Btk horizon); slightly effervescent; unit is not faulted by primary or secondary faults in underlying deposits; grades upward into unit 10; clear smooth basal contact; (TECTONIC SCARP-DERIVED PROXIMAL COLLUVIUM).

Unit 8: Late Pleistocene fissure fill / fault gouge. Reddish yellow (7.5YR 6/6) SAND WITH GRAVEL. Fine to coarse sand; subrounded to subangular gravel as much as 10 cm; 10 to 20% gravel; map unit consists of several separate, triangular-shaped bodies along the primary fault near station 25 and associated with secondary faults near stations 21 and 24 m (northern wall only); contains gravel clasts having vertical orientations that are sandstone clasts similar to those in unit 2 and $CaCO_3$-rich sand similar to that of unit 6; all subunits appear to be basal parts of overlying unit 9; poorly sorted; dry, hard; clear irregular lateral margins.

Unit 7: Late Pleistocene fault gouge. Reddish yellow (7.5YR 6/6) SAND WITH GRAVEL. Fine to coarse sand; subrounded to subangular gravel as much as 30 cm but commonly < 10 cm; 10 to 20% gravel; map unit consists of two separate, near-vertical bodies, one along primary fault near station 25 m and one associated with secondary fault near station 21 m; both contain gravel clasts having vertical orientations; eastern sub-unit (within primary fault zone) is pervasively sheared and contains sandstone clasts similar to those in unit 2; western subunit (near secondary fault zone) does not appear to be sheared, and contains only subangular clasts of $CaCO_3$-rich sand similar to unit 6; poorly sorted; dry, hard; clear smooth lateral margins.

Unit 6: Middle to Late(?) Pleistocene alluvium/colluvium. Pink (7.5YR 8/4) CLAYEY SAND. Fine to coarse sand; subrounded to subangular gravel as much as 15 cm; 5% gravel, locally within discontinuous beds that dip gently eastward toward the primary fault (on southern wall near station 24 m) or toward the secondary fault (on northern wall near station 20 m); poorly sorted; dry, hard; contains stage III calcium carbonate (soil Bkm horizon); pervasive calcium carbonate throughout deposit; strongly effervescent; unit is sheared and faulted adjacent to faults near stations 21 and 24 m; gradual irregular basal contact.

Unit 5: Middle to Late(?) Pleistocene alluvium/colluvium. Very pale brown (10YR 7/3) SAND WITH GRAVEL. Fine to coarse sand; subrounded to subangular gravel as much as 20 cm, with larger clasts adjacent to primary fault near station 25 m and adjacent to secondary fault near station 21 m; 10% gravel directly west of primary fault zone near station 25 m and directly west of secondary fault zone near station 21 m; lower percentage (<5%) of gravel elsewhere; massive; poorly sorted; dry, hard; contains stage III calcium carbonate (soil Bkm horizon); effervescent; unit is sheared and faulted adjacent to faults near stations 21 and 25 m; clear smooth basal contact.

Unit 4: Middle Pleistocene alluvium. Very pale brown (10YR 7/3) SILTY SAND. Fine to coarse sand; subrounded to subangular gravel as much as 5 cm; <5% gravel; massive; dry, hard; contains subhorizontal and subvertical stringers of calcium carbonate (likely related to vadose groundwater precipitation); effervescent; clear wavy basal contact.

Unit 3: Middle Pleistocene alluvium. Light brown to brown (7.5YR 5/4 to 7.5YR 6/4) SANDY GRAVEL, grading upward to very pale brown (10YR 7/3) GRAVELLY SAND. Fine to coarse sand; subrounded to subangular gravel as much as 30 cm in lower part; effervescent; massive; dry, hard; basal contact not observed.

Unit 2: Middle Pleistocene alluvium. Strong brown (7.5 YR 6/4 to 7.5YR 6/6) pebble to boulder GRAVEL; 40 to 60% subrounded to subangular gravel clasts as much as 36 cm; locally map unit contains finer gravel sub-units with clasts < 10 cm, and very coarse gravel sub-units with clasts ranging from 10 to 36 cm; lower exposures loose; upper part pedogenically modified and cemented pebbly sandstone and conglomerate; strongly effervescent; extensively bioturbated; stage III pedogenic calcium carbonate horizon near top. Lower part includes irregular bodies of gravel, loose to well cemented with calcium carbonate; carbonate appears concentrated in subvertical pipes and fingers below the pedogenic carbonate and in subhorizontal bedding; gravel clasts locally cemented by white (N 8/0) 1- to 2-mm-thick calcium carbonate rinds. Clast and matrix-supported gravel exhibits horizontal- to low-angle cross-stratified beds to 2 m thick; well bedded; thinly bedded to laminated in sets 3 to 5 cm thick; abrupt basal contact.

Unit 1: Middle Pleistocene intermixed alluvium and loess. Strong brown (7.5YR 4/6 to 7.5YR 5/6) SAND, SILT, and CLAY (divided into upper (1b) and lower (1a) sub-units). Sub unit 1b: Pinkish white (7.5YR 8/2 to reddish yellow (7.5YR 6/6) SANDY SILT with CLAY; slightly hard; moderately effervescent to noneffervescent; subvertical carbonate filled fractures taper from 4 cm to fine cracks as much as 55 cm long are exposed between stations 33 and 32 m and between stations 39 and 40 m; clear smooth basal contact. Sub-unit 1a: Reddish yellow (7.5YR 6/6) to strong brown (7.5YR 4/6) CLAYEY SILT; dense, weakly to noneffervescent; locally contains 1 cm diameter cicada burrow casts; locally contains 3- to 30-cm-thick silty sand beds with low-angle cross beds; poorly sorted; 10-15% of lower unit locally; base not exposed.

APPENDIX B: FIELD-DETERMINED SOIL CHARACTERISTICS, TRENCH T-1

Description of Pedon 1B, east of Sangre de Cristo fault. Symbols and nomenclature after Birkeland (1999), Munsell (1992) and Soil Survey Staff (1993). Soil descriptions by S. Connell on June 12, 2003.

Horizon	Depth (cm)	Color (dry/*moist*)	Texture	Structure	dry sticky	Moist plas	Clay	Gravel (%)	Pores	$CaCO_3$	Bndry	Cmnts
A	0-3	7.5YR 4/4 *7.5YR 3/4*	SL	Sg	lo ss	lo ps	n.o.	<1	n.o.	eo	as	Unit 11
Btk1	3-14	7.5YR 4/4 *7.5YR 3/3*	SCL	2m-c sbk	so	lo	1nco	<2	1vf	es (dissem)	cs	Unit 11
Btk2	14-26	7.5YR 4/3 *7.5YR 3/3*	SCL	2m sbk	so	so	1nbr	<2	1f	es (l)	cs	Unit 11
Bk3	26-43	7.5YR 5/2 *7.5YR 4/4*	LS	1m sbk	sh	fi	v1nco	<5	1f-m	es (l)	cs	Unit 11
2Bk1b	43-59	7.5YR 8/1 *7.5-10YR 7/3*	LS	1m abk	sh ss	fr po	n.o.	10	1f-m	ev (III)	cs	Unit 2
2Bk2b	59-101	7.5YR 8/1-2 *7.5YR 5/3*	SL	sg-1m sbk	lo so	lo po	n.o.	30-40	n.o.	ev (II+)	cw	Unit 2
2Bk3b	101-113	7.5YR 8/1 *7.5YR 8/2-7/4*	SL	sg	lo so	lo po	n.o.	10	n.o.	ev (II+)	as	Unit 2
2Bkmb	113-117	7.5YR 7/4 *7.5YR 5/4*	LS	m	h sh	vfi po	n.o.	5	1vf 2co	ev (II+)	as	Unit 2
2Bk1b	117-162	7.5YR 8/1 *7.5YR 8/2-7/4*	LS	sg	lo so	lo po	v1nco	40	n.o.	ve (l)	as	Unit 2
2Btk2b	162-226	7.5YR 5/4 *7.5YR 4/3*	LS	sg	lo so	lo po	1mkpf 1nco	60	n.o.	es (l+)	aw	Unit 2
3Btb	226-246	7.5YR 4/6 *7.5YR 4/4*	C	2fpr 1m-cabk	sh s	fr mp-p	3mkpfpo	0	2f	eo	cs	Unit 1
3Bb1	246-267	7.5YR 5/6 *7.5YR 4/6*	C	2m-cabk	sh s	vfr mp-p	n.o.	0	2co 1f	eo	cs	Unit 1
3Bb2	267-279	7.5YR 5/6-4 *7.5YR 4/4*	C	2mabk	sh s	vfr mp-p	v1npo	0	1vf	eo	n.o.	Unit 1

Description of Pedon 1C, west of Sangre de Cristo fault. Symbols and nomenclature after Birkeland (1984), Munsell (1992) and Soil Survey Staff (1993). Soil descriptions by S. Connell and D. Love.

Horizon	Depth (cm)	Color (dry/*moist*)	Texture	Structure	dry sticky	Moist plas	Clay	Gravel (%)	Pores	$CaCO_3$	Bndry	Cmnts
B	0-11	7.5YR 4/4 *7.5YR 3/3*	SiCL	2-3c abk	sh ss	vfr ps	Vlnco	1-2	1f	eo	cs	Unit 11
Btk1	11-29	7.5YR 5/4 *7.5YR 4/3-4*	SiCL	2-3m-c sbk	sh s	vfr ps-mp	vlnpo 1ncopf	<2	1f	ve-e	cs	Unit 11
Btk2	29-44	7.5YR 5/4 *7.5YR 5/4*	C	2m-c abk 3fpr	sh s	vfr mp	1npopf	<2	2vf-f	e (l)	cs	Unit 10
Btk3	44-66	7.5YR 6/4 *7.5YR 5/4*	C	3fpr 2m abk	h s	fr mp	1npf	<2	2vf-f	es (l+)	gs	Unit 10
Btk4	66-101	7.5YR 6/6 *7.5YR 5/6*	C	3fpr 2m-c abk	h s	fr mp	1nbrpf	<2	1vf-f	e (l+)	cs	Unit 10
Btk5	101-125	7.5YR 6/6 *7.5YR 5/6*	C	2m-c abk	sh s	vfr mp	2mkbrpf	<5	1vf	ve (l+)	aw	Unit 9
2Bkmb1	125-145	7.5YR 8/4 *7.5YR 7/4*	C	1f-m abk	h ss	vfr mp	n.o.	<2	2vf-f	ev (III)	cw	Unit 6
2Bkmb2	145-197	10YR 7/3 *7.5YR 7/4*	C	1f abk	sh ss	vfr mp	n.o.	<2	2f	ev (III)	gi	Unit 6
2Bkmb3	197-215	10YR 7/3 *10YR 6/6*	C	1f-m abk	so ss	vfr mp	n.o.	<5	1vf	ev (III)	cw	Unit 5
2Bkmb4	215-233	10YR 8/3 *10YR 7/3*	SCL	1f-m abk sbk	h ss	vfr ps	1npf	<5	n.o.	ev (III)	ci	Unit 4
3Bkb	233-248	7.5YR 6-5/4 *7.5YR 4/3*	SCL	sg-1f sbk	sh ss	vfr ps	v1copf	20	n.o.	e	n.o.	Unit 3

PLATE 9: TRENCH PROFILE – SANGRE DE CRISTO FAULT

KEITH I. KELSON, SEAN D. CONNELL, DAVE W. LOVE, AND PAUL W. BAUER

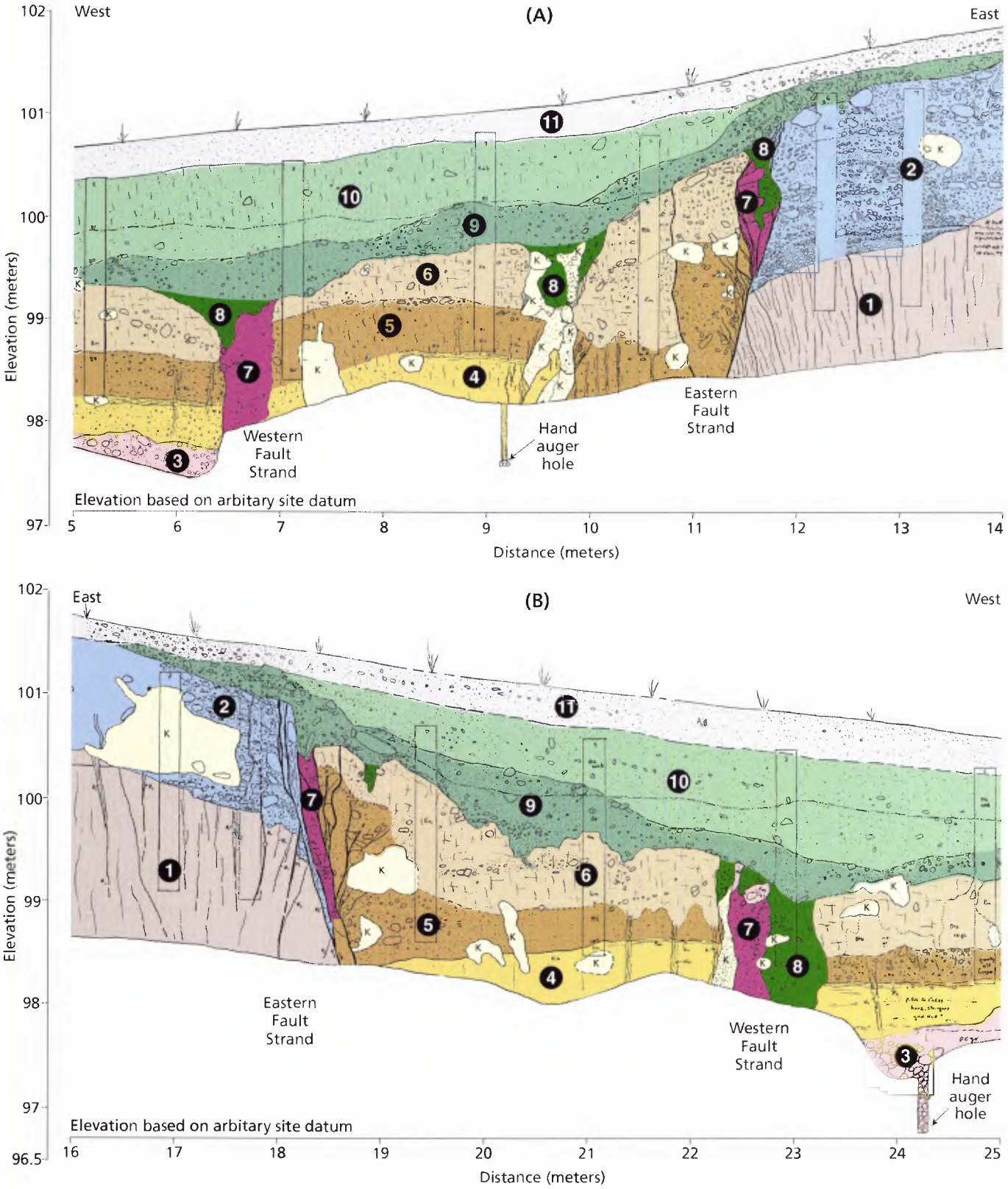

PLATE 9. Detailed trench profiles of the Sangre de Cristo fault exposed in (a) northern wall and (b) southern wall of trench T-1, Taos Pueblo site. For discussion and unit descriptions, see Kelson et al. (2004, this volume) and Appendix A therein. K = krotovina (bioturbation).

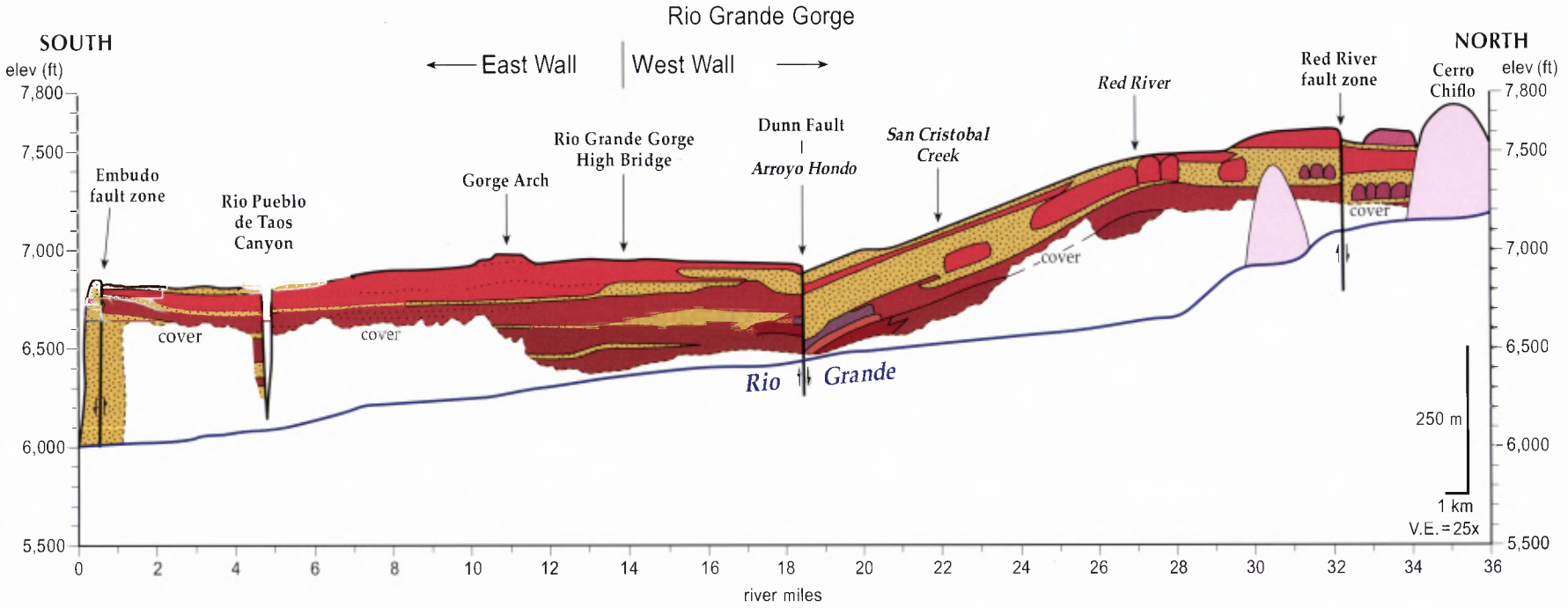

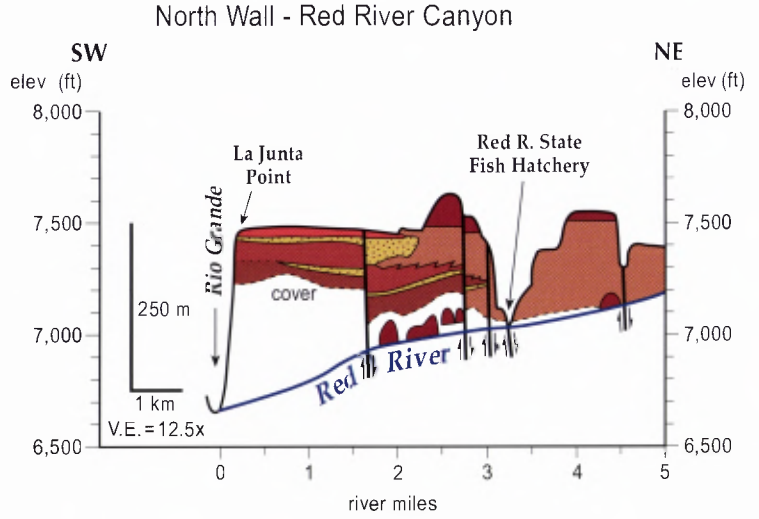

PLATE 10. Composite longitudinal profiles and cross sections of the volcanic stratigraphy exposed in the Rio Grande and Red River gorges. The data were compiled from scanned plates from the M.S. theses of Peterson (1981) and Leininger (1982). See roadlog references for complete citations.